**International Journal of Material and Mechanical Engineering, 2012, 1: 71-88**
Published Online July 2012

www.ijm-me.org



# Revisiting the Spinning Top

Christopher G. Provatidis
Department of Mechanical Engineering, National Technical University of Athens, Athens, Greece
Email: cprovat@central.ntua.gr

**(Abstract)** This paper revisits the problem of a spinning top in a uniform gravitational field when one point on the symmetry axis is fixed in space. It is an instructive and synthetic work of which the theoretical part includes all necessary issues to formulate the full differential equations governing the general motion of the spinning top under arbitrary initial conditions. Both Euler and Lagrange formulations are discussed. Moreover, closed form analytical solutions are derived for the regular precession and the nutation. The numerical integration of the equations was achieved using the standard Runge-Kutta scheme ODE45 available in MATLAB®, which was initially applied to the totality of Euler's equations and then to Lagrange's equations. Also, in house RK2 and RK4 Runge-Kutta as well as Crank-Nicolson schemes were applied in conjunction with the constraint for energy conservation. The quality of the numerical solution was evaluated by testing the conservation of total energy as well as angular momenta in the form of residuals in the corresponding Euler's dynamic equations.

**Keywords:** spinning top; symmetrical gyroscope; Euler's equations; Lagrange's equations.

## 1. INTRODUCTION

Symmetric spinning top is a case studied by Lagrange in 1788 [1]. After 110 years, in 1897-1898 Klein and Sommerfeld [2,3] published two volumes, whereas in 1897 Klein separately published a shorter monograph on the mathematical theory of the top [4]. In the eastern world literature, one of the oldest papers is probably due to Appel'rot (1894) [5]. Historical books of general interest are [6,7], whereas another book by Gould [8] includes 367 references until early 1970s. Explicit integration of motion equations, to give the nutation in terms of elliptic integrals is cited in the aforementioned books at the end of nineteenth century [3,4] as well as in Whittaker [9]; some useful explanations are due to Zaroodny [10].

Older standard books of physics and classical dynamics [11-14] include analytical formulas for nutation, whereas recent physics standard textbooks [15,16] limit their discussion only to the case of regular precession. There is no doubt that the spinning top, as a toy, keeps its fascination from little children to adults. A simple internet search reveals many references concerning the spinning tops and gyros as if they were "magical" instruments that defy gravity. Even the renowned mathematician Michèle Audin has used the term "mysterious (?)" when referring to Kowalevski case in the introduction of her book [17]. It is worth-mentioning that, in 1889, Kovalevskaya showed that the rigid body motion was integrable under certain conditions concerning the ratio (1:2) of the principal momenta between other parameters; her work was so remarkable that it won her the Bordin prize (1888) [12,34-37]. Besides the toy, there are many industrial applications such as navigation of the closely related gyroscope. However, a detailed literature survey on the gyroscope and its applications is outside the scope of this paper.

The integrability of Euler's equations describing the motion of a spinning top has become a matter of intensive research within the last fifteen years. In brief, the numerical solution may sometimes not fulfill the law of energy conservation or may suffer from "gimbal lock" singularities concerning the Euler angles [17-19]. In the regime of numerical analysis, the first paper in the western literature referring (among others) to the numerical integration of the differential equations of a spinning top is probably due to Gorn [20,p.79]. Later, McGill and Long [21] studied the case of an unsymmetrical rigid body. Simo and associates have developed numerical schemes to preserve energy and momentum [22,23] and papers therein. Ratiu and Moerbeke [24] have discussed the same matter with main emphasis put on the symplectic structure of the motion. Historical references have been recently given by Romano [25], whereas most recent publications are [26-31].

Despite the abovementioned progress, the applicability of general purpose numerical integration schemes remains an open issue. This paper contributes in this direction by developing two variations of the differential equations and then implementing standard MATLAB functions such as ODE45, which is a code based on a pair of one-step explicit Runge-Kutta formulas. The study investigates the performance of this time-integrator for the conservation of the energy and the angular momentum. For the sake of briefness, the study reduces to the symmetrical spinning top.

## 2. EQUATIONS OF MOTION

### 2.1. Euler's equations

The top is a rigid body fixed at the point O. Its position (orientation) at any instant can be fully described by three Euler angles. Following Targ [13], the fixed co-ordinate system (space axes) is denoted by ($x_1$,$y_1$,$z_1$) whereas the rotating system (body axes) is denoted by ($x$,$y$,$z$). The unit vectors for the space and body systems are denoted by $(\mathbf{i}_1, \mathbf{j}_1, \mathbf{k}_1)$ and $(\mathbf{i}, \mathbf{j}, \mathbf{k})$, respectively. According to the original definition, first we define the *line of nodes* (ON) as the intersection between the O$x_1y_1$ and the O$xy$ coordinate planes; in other words, the line of nodes is the line perpendicular to both $z_1$ and $z$ axis and therefore it always lies on the fixed horizontal plane O$x_1y_1$. The unit vector along (ON) is denoted by $\mathbf{n}_0$ and it is chosen so as the system ($\mathbf{k}_1$,$\mathbf{k}$,$\mathbf{n}_0$) is right-handed. As usual, we define the Euler angles as:

- $\phi$ is the *azimuthal* angle between the $x_1$-axis and the line of nodes (ON).
- $\theta$ is the *inclination* (lean) angle between the $z_1$-axis and the $z$-axis.
- $\psi$ is the *spin* angle between the line of nodes (ON) and the $x$-axis.

Different authors may use different sets of angles to describe these orientations, or different names for the same angles, leading to different conventions (see, for example, Berry and Shukla [32] or the textbook by Hay [33]).

Let C be the center of mass of the spinning top, which is taken along the $z$-axis at a distance $l$ from the fixed origin O. The two first Euler angles ($\phi$ and $\theta$) are directly related to the polar angles $\phi_p$ and $\theta_p$ (known as two of the usual spherical coordinates: $\phi_p, \theta_p, r_c = l$) of the axis, whose direction is the unit vector $\mathbf{k}_1$, as follows: $\phi_p = \phi - \pi/2$ and $\theta_p = \theta$. The angle $\psi$ describes the rotation of a material rotation of a material point P about the axis of the top, measured relative to the intersection of the top with the instantaneous constant $\phi_p$–plane. The latter is better understood if at time $t$ = 0 we assume the body $x$-axis to coincide with the line of nodes (ON); at this case the plane (O$yz$) is perpendicular to the plane (O$x_1y_1$) and it intersects the circular cross section at the point $P_0$ (**Figure 1**). Irrelevant to a possible nutation, it is obvious that at a later instant $t$, the material point P will have rotated along the circle (transverse to the body $z$ axis) exactly by the Euler angle $\psi$.

Since the spinning top has a fixed point at O, at every instant the motion of the rigid body is a pure rotation about the instantaneous vector of the angular velocity **ω** (along a line OΩ, not shown), which can be expressed in terms of the Euler angles as follows: $\omega_\phi = \dot{\phi}$, $\omega_\theta = \dot{\theta}$, $\omega_\psi = \dot{\psi}$. In more details, $\omega_\phi$ is along the space $z_1$ axis, $\omega_\theta$ is along the line of nodes (ON), while $\omega_\psi$ is along the body $z$ axis. As known [1; 12 p.174], adding these components of the separate angular velocities, the components $(\omega_x, \omega_y, \omega_z)$ of **ω** with respect to the rotating body axes O$xyz$ are given by:

$$\begin{aligned} \omega_x &= \dot{\phi}\sin\theta\sin\psi + \dot{\theta}\cos\psi, \\ \omega_y &= \dot{\phi}\sin\theta\cos\psi - \dot{\theta}\sin\psi, \\ \omega_z &= \dot{\phi}\cos\theta + \dot{\psi}. \end{aligned} \tag{1}$$

If now the body axes ($xyz$) are taken as the principle axes (123) relative to the reference point O, with moments of inertia ($I_1$, $I_2$, $I_3$), the abovementioned components of **ω** are now denoted by ($\omega_1, \omega_2, \omega_3$). Then, the totality of Euler equations (kinematic and dynamical) is given as follows:

i) Kinematic Euler equations

$$\omega_1 = \dot{\phi}\sin\theta\sin\psi + \dot{\theta}\cos\psi, \tag{2a}$$

$$\omega_2 = \dot{\phi}\sin\theta\cos\psi - \dot{\theta}\sin\psi, \tag{2b}$$

$$\omega_3 = \dot{\phi}\cos\theta + \dot{\psi}. \tag{2c}$$

ii) Dynamical Euler equations

$$I_1\dot{\omega}_1 - (I_2 - I_3)\omega_2\,\omega_3 = M_1, \tag{3a}$$

$$I_2\dot{\omega}_2 - (I_3 - I_1)\omega_3\,\omega_1 = M_2, \tag{3b}$$

$$I_3\dot{\omega}_3 - (I_1 - I_2)\omega_1\,\omega_2 = M_3. \tag{3c}$$

A rigorous proof of Equations (3) is given in Appendix A. The transformation of the angular velocities from the body to the space (fixed) system is given in Appendix B.

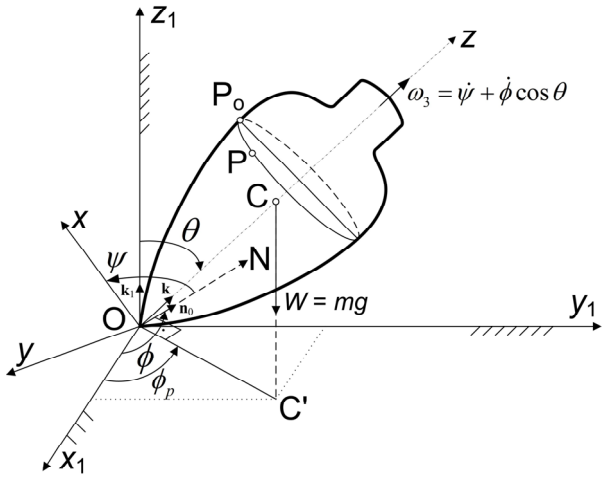


**Figure 1.** Euler angles of a spinning top.

Equations (2) and (3) provide the general mathematical formulation for the motion of the rigid body having one fixed point. In the general case of unsymmetrical shape, their solution constitutes a difficult mathematical problem [13].

In the particular case of a symmetrical spinning top, it is convenient to choose the *z*-axis to be the axis of symmetry, so as $I_1 = I_2 \neq I_3$. In this case the solution becomes easier. In fact, the position vector for the center of gravity C is given as follows:

Space system ($Ox_1y_1z_1$):

$$\mathbf{r}_{1,C} = l\left[\sin\phi\sin\theta \quad -\cos\phi\sin\theta \quad \cos\theta\right]^T \tag{4a}$$

Body system ($Oxyz$):

$$\mathbf{r}_C = \left[0 \quad 0 \quad l\right]^T \tag{4b}$$

Therefore, the components of the moment ($M_1$, $M_2$, $M_3$) in the right-hand-side of Eq(3abc) are produced by the moments of the weight with respect to the origin O [cross product $\mathbf{r}_C \times (-m\mathbf{g})$], which is then projected onto the body *x*-, *y*-, and *z*-axes, respectively. In the particular case of a spinning top in a constant gravitational field, with respect to the world system the weight *mg* (acting at the center C) is the vector $mg\left[0 \quad 0 \quad -1\right]^T$. Considering the transformation matrix **A** obtained after the abovementioned three rotations about the $z_1$, ON and *z* axes, respectively [12, p.153]:

$$\mathbf{A} = \begin{pmatrix} \cos\phi\cos\psi - \sin\phi\cos\theta\sin\psi & \sin\phi\cos\psi + \cos\phi\cos\theta\sin\psi & \sin\theta\sin\psi \\ -\cos\phi\sin\psi - \sin\phi\cos\theta\cos\psi & -\sin\phi\sin\psi + \cos\phi\cos\theta\cos\psi & \sin\theta\cos\psi \\ \sin\phi\sin\theta & -\cos\phi\sin\theta & \cos\theta \end{pmatrix}, \tag{5}$$

the projections of the weight onto the axes of the body system are given by the matrix product $mg \cdot \mathbf{A} \cdot \left[0 \quad 0 \quad -1\right]^T$, whence the torques appearing in (3) are expressed by

$$\begin{Bmatrix} M_1 \\ M_2 \\ M_3 \end{Bmatrix} = mgl \begin{Bmatrix} \sin\theta\cos\psi \\ -\sin\theta\sin\psi \\ 0 \end{Bmatrix} \tag{6}$$

**Remarks**

1) We notice that the Euler angle $\psi$ appears in both the kinetic and dynamical expressions (2) and (3) as well as in (6).
2) Since $M_3 = 0$, by virtue of the condition $I_1 = I_2$ Eq(3c) implies that $\dot{\omega}_3 = 0$, which means that the component $\omega_3$ is a constant.
3) A torque with components $M_1$ or $M_2$ will cause both $\omega_1$ and $\omega_2$ to change without affecting $\omega_3$.
4) Whatever the external loading is, the initial conditions at the instant $t = 0$ are the following six quantities:

$$\left(\phi_0, \dot{\phi}_0\right), \left(\theta_0, \dot{\theta}_0\right) \text{and} \left(\psi_0, \dot{\psi}_0\right), \tag{7}$$

from which the angles $\phi_0$ and $\psi_0$ are needed only for reference (they do not affect the visual orientation of the symmetrical spinning top). In other words, the mechanical behavior is determined by the four initial conditions: $\left(\dot{\phi}_0, \theta_0, \dot{\theta}_0, \dot{\psi}_0\right)$, which determine the energy (see below Eq(18)).

5) The measure of the vector of the angular velocity $\boldsymbol{\omega}\left(\omega_1, \omega_2, \omega_3\right)$ is given by:

$$\begin{aligned} \|\boldsymbol{\omega}\| &= \left(\omega_1^2 + \omega_2^2 + \omega_3^2\right)^{1/2} \\ &= \left(\dot{\phi}^2 + \dot{\theta}^2 + \dot{\psi}^2 + 2\dot{\phi}\dot{\theta}\cos\theta\right)^{1/2} \end{aligned} \tag{8}$$

6) The angle $\alpha$ between the abovementioned vector $\boldsymbol{\omega}$ and the body *z* axis is determined by the direction cosine $\omega_3 / \|\boldsymbol{\omega}\|$, which by virtue of Eqs(2c) and (8) becomes:

$$\cos\alpha = \frac{\left(\dot{\phi}\cos\theta + \dot{\psi}\right)}{\left(\dot{\phi}^2 + \dot{\theta}^2 + \dot{\psi}^2 + 2\dot{\phi}\dot{\theta}\cos\theta\right)^{1/2}} \tag{9}$$

## 2.2. Lagrange's equations

In terms of the instantaneous angular velocity $\boldsymbol{\omega}$ of the rigid body that moves about the fixed point O, the kinetic energy can be computed according to the formula $T = 1/2\, I_{O\Omega}\omega^2$, where $I_{O\Omega}$ is the variable moment of inertia with respect to the instantaneous axis of rotation OΩ. In terms of the components of the angular velocity $\boldsymbol{\omega}\left(\omega_1, \omega_2, \omega_3\right)$ in the body system, the kinetic energy is given according to the formula

$$T = \frac{1}{2}\left(I_1\omega_1^2 + I_2\omega_2^2 + I_3\omega_3^2\right) \tag{10}$$

Substituting (2) into (10) and considering a symmetrical top, i.e. $I_1 = I_2$, the latter takes the form:

$$T = \frac{I_1}{2}\left(\dot{\theta}^2 + \dot{\phi}^2 \sin^2\theta\right) + \frac{I_3}{2}\omega_3^2 \tag{11}$$

Also, the potential energy is given by

$$V = mgl\cos\theta \tag{12}$$

Following Targ [13, pp. 518-519], the Lagrange's equations are written as follows:

$$\begin{aligned} \frac{d}{dt}\left(\frac{\partial T}{\partial \dot{\phi}}\right) - \frac{\partial T}{\partial \phi} &= Q_\phi \\ \frac{d}{dt}\left(\frac{\partial T}{\partial \dot{\theta}}\right) - \frac{\partial T}{\partial \theta} &= Q_\theta \\ \frac{d}{dt}\left(\frac{\partial T}{\partial \dot{\psi}}\right) - \frac{\partial T}{\partial \psi} &= Q_\psi \end{aligned} \tag{13}$$

Alternatively, we can consider the Lagrangian $L = T - V$ and take the equivalent form: $\frac{d}{dt}\left(\frac{\partial L}{\partial \dot{q}}\right) - \frac{\partial L}{\partial q} = M_q$ . Substituting (11) into (13) and assuming that the only load is due to the weight $W=mg$ of the spinning top, the right-hand sides ( $Q_\phi$ , $Q_\theta$ , $Q_\psi$ ) of Eq(13) correspond to the moments $M_{z_1} = 0$, $M_{ON} = Wl\sin\theta$ (ON= line of nodes) and $M_z = 0$, respectively. As a result, Eq(13) becomes:

$$\frac{d}{dt}\left(I_1\dot{\phi}\sin^2\theta + I_3\omega_3\cos\theta\right) = 0 \ , \tag{14a}$$

$$I_1\ddot{\theta} - I_1\dot{\phi}^2\sin\theta\cos\theta + I_3\omega_3\dot{\phi}\sin\theta = mgl\sin\theta \tag{14b}$$

$$I_3\frac{d\omega_3}{dt} = 0 \tag{14c}$$

One can notice that Eq(14a) and Eq(14b) do not include the Euler angle $\psi$ .

It is worth-mentioning that (14a) dictates that the value of the component of the angular momentum towards the space $z_1$-axis is a constant (*first invariant* of the system), i.e

$$p_\phi = \partial L/\partial\dot{\phi} = I_1\dot{\phi}\sin^2\theta + I_3\omega_3\cos\theta = c_1 \ , \tag{15a}$$

where the constant value $c_1$ in (15a) is directly determined in terms of three initial conditions ( $\dot{\phi}_0, \theta_0, \dot{\psi}_0$ ), mentioned in (7), as follows:

$$c_1 = I_1\dot{\phi}_0\sin^2\theta_0 + I_3\left(\dot{\phi}_0\cos\theta_0 + \dot{\psi}_0\right)\cos\theta_0 \ , \tag{15b}$$

Equation (14c) depicts that $\omega_3$ is a constant, which can be calculated in terms of *three* initial conditions ( $\dot{\phi}_0, \theta_0, \dot{\psi}_0$ ) using the kinematic Euler equation (2c), i.e.

$$\omega_3 = \dot{\phi}_0\cos\theta_0 + \dot{\psi}_0 \tag{16}$$

Obviously, for any instant $t > 0$ the component $\omega_3$ is given by Eq(2c). Equation (2c) depicts that the aforementioned material point P undertakes a *relative* rotation around the rotating $z$-axis and it also undertakes the *transport* rotation $\dot{\phi}\mathbf{k}_1$ (namely its projection $\dot{\phi}\cos\theta$ along the $z$-axis).

Since $\omega_3$ is a constant, the *second invariant* of the system (angular momentum towards the body $z$ axis) is:

$$p_\psi = \frac{\partial L}{\partial\dot{\psi}} = I_3\omega_3 \tag{17}$$

Unlike Euler's equations, these equations define the motion only of a symmetrical body for which $I_1 = I_2$ . However, they are simpler than the totality of Euler's dynamic and kinematic equations [13, p. 519].

Usually, a criterion to test the accuracy of the numerical integration is the energy conservation, which is given by the form ($E = T + V$) as follows:

$$E = \frac{1}{2}I_1\left(\dot{\theta}^2 + \dot{\phi}^2\sin^2\theta\right) + \frac{1}{2}I_3\omega_3^2 + mgl\cos\theta = c_2 \tag{18}$$

As previously, the value $c_2$ in (18) is directly determined in terms of the initial conditions (7) and particularly it requires *four* of them ( $\dot{\phi}_0, \theta_0, \dot{\theta}_0, \dot{\psi}_0$ ).

## 3. A CRITICAL REVIEW ON THE MOTION OF THE SPINNING TOP

In the general motion of the spinning top the inclination (lean) angle $\theta$ varies in time. The latter motion is defined as "nutation". However, the case of "no nutation", which is also called "regular precession", appears a particular interest. At this point it is worth-mentioning that given the six initial conditions [Eq(7)] the time history in the orientation of the spinning top can be calculated in an deterministic way. It was previously mentioned that two of the initial conditions, that is the initial angles $\phi_0$ and $\psi_0$ do not play any significant role since they are only *reference* values. In other words, the history in the position of the spinning top depends on the four initial conditions $\dot{\phi}_0, \theta_0, \dot{\theta}_0, \dot{\psi}_0$ . The aforementioned four initial conditions determine the three system invariants, which are the component of the angular momentum along the $z_1$ axis

( $p_\theta \equiv c_1$ ), the component of the angular momentum along the *z* axis ( $p_\psi \equiv I_3\omega_3$ ) and the total energy ( $E = c_2$ ).

### 3.1. Constant inclination angle

When the inclination angle is constant, we then refer to the abovementioned "regular" or "steady" or "smooth" precession.

The investigation of motions under gravity in which the axis of the top makes a constant angle with the vertical has been reported for example by Hay [33, pp. 91-94]. However, since Hay [33] uses a different body-fixed coordinate system, it makes sense to adapt his approach to our traditional *xyz* body system.

The assumption of a constant angle $\theta$ , whence $\dot\theta = 0$ , causes Eq(2a), (2b) and (2c) to give:

$$\omega_1 = \dot\phi \sin\theta \sin\psi\,, \quad \omega_2 = \dot\phi \sin\theta \cos\psi\,, \quad \omega_3 = \dot\phi \cos\theta + \dot\psi\,. \tag{19}$$

For this particular case, we designate $p = \dot\phi$ for the precession, and $s = \dot\psi$ for the spin.

Multiplying (3a) by $\cos\psi$ and (3b) by $\sin\psi$ , then subtracting by parts and assuming that ($I_1 = I_2$), one obtains:

$$\left[\left(I_3 - I_1\right)\cos\theta\, p^2 + I_3 sp - mgl\right]\sin\theta = 0, \tag{20a}$$

Substituting (20a) into the abovementioned (3b) already having been multiplied by $\sin\psi$, one obtains:

$$\left(I_1 \dot p \cos\psi\right)\sin\theta = 0 \tag{20b}$$

Lastly, Eq(3c) becomes:

$$\dot p \cos\theta + \dot s = 0\,. \tag{20c}$$

Equations (20a), (20b) and (20c) are identical with those obtained by Hay [33] in a different way.

Again, the totality of Equation (3) is given by equations (20). Below, we distinguish two cases.

1) One solution of Eq(20) is $\theta = 0$ . In this case the axis of the top is vertical, and the top is said to be "sleeping". Then, (20c) becomes $\dot p + \dot s = 0$ , which means that the precession is equal and opposite to the spin.
2) If $\theta$ is not equal to zero, then $\sin\theta$ can be eliminated in (20a,b). Therefore, (20b) yields $\dot p = 0$ whereas (20c) then yields $\dot s = 0$ . In other words, *p* = constant, *s* = constant. Equation (20a) is a relation among the three constants *p*, *s* and $\theta$ . Hence it appears that we may assign arbitrarily values for two of these constants and there will exist a corresponding motion of the top with $\theta$ a constant. Following Hay [33,p.94], Eq(20a) can be solved in *s*:

$$s = \frac{mgl}{I_3 p} - \frac{\left(I_3 - I_1\right) p \cos\theta}{I_3} \tag{21a}$$

Equation (21a) offers the dependency of the spin (*s*) of the precession (*p*) and the inclination angle ( $\theta$ ). In particular, the precession appears in both the denominator and the nominator. If the precession is small (*p*<<), we note from (18a) that the second term vanishes whereas the first one becomes large and it is approximated by the value

$$s \cong \frac{mgl}{I_3 p} \tag{21b}$$

Moreover, whatever the value of the precession is, if the long *z* axis of the top is horizontal ( $\theta = \pi/2$ , i.e. $\cos\theta = 0$ ), equation (21b) is not an approximation but an exact solution and, if solved in *p* we obtain:

$$\text{For } \theta = \pi/2: \qquad p = \frac{mgl}{I_3 s} \tag{21c}$$

which is the well-known from textbooks of physics [15,16]. While Eq(21c) is valid for a horizontal top under any conditions, for any other inclination it may hold under the abovementioned conditions.

Although Eq(20a) is a quadratic equation in *p*, it is not offered to determine the precession angular velocity *p* as is, because *s* depends on *p* according to Eq(2c). Therefore, substituting Eq(2c) into Eq(20a) one finally obtains:

$$\left(I_1 \cos\theta\right) p^2 - \left(I_3\omega_3\right) p + mgl = 0, \quad \theta \neq \pi/2 \tag{22}$$

Equation (22) constitutes the sufficient and necessary condition to achieve regular precession (no nutation). It is mentioned that Eq(22) can be also obtained from Eq(14b) putting $\ddot\theta = 0$ and eliminating $\sin\theta$ in both left and right parts.

In more details, when $\theta \neq \pi/2$ , the quadratic equation (22) is valid and its discreminant is

$$D = \left(I_3\omega_3\right)^2 - 4 I_1 lmg \cos\theta \tag{23}$$

As a real solution requires $D \geq 0$ , a "conditio sine qua non" for the axial angular velocity $\omega_3$ to achieve an inclination angle $\theta$ is:

$$\omega_3^2 \geq \frac{4 I_1 lmg \cos\theta}{I_3^2} \tag{24}$$

Provided Eq(24) is valid ( $D \geq 0$ ), the two roots of (22) are given by

$$p = \frac{I_3\omega_3}{2 I_1 \cos\theta} \pm \sqrt{\left(\frac{I_3\omega_3}{2 I_1 \cos\theta}\right)^2 - \frac{lmg}{I_1 \cos\theta}} \tag{25a}$$

Therefore, the plus and minus sign in (25a) produce two solutions: the so-called "fast" precession and the "slow" precession solutions.

In more details, equation (25a) can be rewritten as follows:

$$p = \frac{I_3\omega_3}{2I_1\cos\theta}\left(1 \pm \sqrt{1-x}\right) \tag{25b}$$

where

$$x = \frac{4lmgI_1\cos\theta}{\left(I_3\omega_3\right)^2} \tag{25c}$$

Under certain circumstances, Eq(25b) can be further simplified. In fact, if it is not only $x \le 1$ but the rotational speed of the spinning top is very large ( $x \ll 1$ ), i.e.

$$I_3\omega_3 >> \sqrt{4lmgI_1\cos\theta}\ , \tag{25d}$$

the root in (25b) is approximated by

$$\sqrt{1-x} \approx 1 - \frac{1}{2}x \tag{25e}$$

In such a case, (25b) implies that the fast and slow precession is approximated by:

Fast precession: $$p_{fast} \approx \frac{I_3\omega_3}{I_1\cos\theta} \tag{25f}$$

Slow precession: $$p_{slow} \approx \frac{mgl}{I_3\omega_3} \tag{25g}$$

**Remarks**

1) One can notice that while the slow precession does not depend on the inclination of the axis of the top (lean angle $\theta$ ) the same does not hold for the fast precession.
2) The slow precession is the one most commonly used experimentally. "In principle, however, one can also obtain a fast precession, although it is difficult to start the gyroscope off with just the right motion to achieve it. In practice, …, the possibility of the fast precession can be ignored" [11, p.683].
3) In the case of slow precession (25g), the value of $p$ corresponding to the negative sign of the radicand in Eq(25a) is very small. Therefore the measure of the angular velocity $\omega = \|\boldsymbol{\omega}\|$ is very close to either of $\omega_3$ and $\dot{\psi}$ (cf. Eq(2c) and Eq(9): $\cos\alpha \approx 1$ ). Therefore, the direction of the vector $\boldsymbol{\omega}$ is very close to the axis of symmetry **k** of the ellipsoid (body $z$ axis).

## 3.2. Nutzation

Nutation is the case according to which the inclination angle varies in time ( $\dot{\theta} \neq 0$ ).

At this point, we closely follow Klein and Sommerfeld [3, p.222] and Goldstein et al. [12, p.213].

Using the two invariant angular momenta ( $p_\phi$ and $p_\psi$ towards space $z_1$ and body $z$ axis, respectively), the total energy can be written as follows:

$$E = \frac{p_\psi^2}{2I_3} + \frac{\left(p_\phi - p_\psi\cos\theta\right)^2}{2I_1\sin^2\theta} + \frac{1}{2}I_1\dot{\theta}^2 + mgl\cos\theta \equiv c_2 \tag{26}$$

Solving (26) in $\dot{\theta}$ , then using the transformation $u = \cos\theta$ , it can be easily verified that the critical (extreme) values of the angle $\theta$ at which the derivative vanishes ( $\dot{\theta} = 0$ : "turning angles") is given by the roots of the following cubic polynomial:

$$f(u) = au^3 + bu^2 + cu + d = 0\,, \tag{27a}$$

with

$$\begin{aligned} a &= 2I_1mgl \\ b &= -\omega_3^2\left(I_3^2 - I_1I_3\right) - 2I_1c_2 \\ c &= 2\left(c_1I_3\omega_3 - I_1mgl\right) \\ d &= 2I_1\left(c_2 - \frac{1}{2}I_3\omega_3^2\right) - c_1^2 \end{aligned} \tag{27b}$$

Dividing by $a$ , (27a) can be also written as follows:

$$u^3 + a_1u^2 + a_2u + a_3 = 0\,, \tag{27c}$$

where

$$a_1 = b/a,\ a_2 = c/a,\ a_3 = d/a. \tag{27d}$$

Equation (27c) is easily solved by introducing the auxiliary variables:

$$Q = \frac{3a_2 - a_1^2}{9},\ R = \frac{9a_1a_2 - 27a_3 - 2a_1^3}{54} \tag{27e}$$

The solution is determined by the sign of the discreminant

$$D' = Q^3 + R^2. \tag{27f}$$

If $D' < 0$ , the roots are given by:

$$\begin{aligned} u_1 &= 2\sqrt{-Q}\cos\left(\frac{1}{3}\beta\right) - \frac{1}{3}a_1 \\ u_2 &= 2\sqrt{-Q}\cos\left(\frac{1}{3}\beta + \frac{2}{3}\pi\right) - \frac{1}{3}a_1 \\ u_3 &= 2\sqrt{-Q}\cos\left(\frac{1}{3}\beta + \frac{4}{3}\pi\right) - \frac{1}{3}a_1 \end{aligned}\ , \tag{27g}$$

with

$$\cos\beta = -R/\sqrt{-Q^3} \tag{27h}$$

Therefore, we obtain one or two roots between the interval [-1,1] and another non-physical root $\left(|u| > 1\right)$ . The two

physically meaningful roots $u_1, u_2$ will yield the *span of angles* of the nutation ( $u_1 \le \cos\theta \le u_2$ ). Obviously, when the roots $u_1, u_2$ are coincident, there is no nutation.

The above analysis can be further simplified if at time $t = 0$ we consider the following initial conditions: $\theta = \theta_0$ , and $\dot{\theta}_0 = \dot{\phi}_0 = 0$ . In this case, the first solution of Eq(27a) is the initial point $\left(u_1 = \cos\theta_0\right)$ , whereas it can be easily proven that for the next solution $u_2$ Eq(27a) becomes:

$$f(u) = (u_1 - u)\left[ aI_1^2\left(1 - u^2\right) + \frac{\left(b + d + c_1^2\right)}{I_1^2}(u_1 - u) \right] \tag{27i}$$

Setting $x = u_1 - u$ and $x_1 = u_1 - u_2$ , the quadratic equation within the brackets in the right hand side of Eq(27i) takes the form:

$$x_1^2 + \overline{p}x_1 - \overline{q} = 0, \tag{27$k$}$$

where

$$\overline{p} = p_\psi^2 / a - 2\cos\theta_0 \quad \text{and} \quad \overline{q} = \sin^2\theta_0, \tag{27$l$}$$

Thus the realistic solution is one root of the quadratic polynomial as follows:

$$x_1 = \frac{-\overline{p} \pm \sqrt{\overline{p}^2 + 4\overline{q}}}{2} \tag{27m}$$

Following Goldstein [12, pp. 215-217], if the kinetic energy of rotation about the body *z* axis is very large compared to the maximum change in potential energy:

$$\frac{1}{2} I_3 \omega_3^2 \gg 2mgl, \tag{28}$$

we speak of the top as being a "fast top". With this assumption we can obtain expressions for the extent of the nutation, the nutation frequency, and the average of the frequency of precession.

Since $\frac{p_\psi^2}{a} = \left(\frac{I_3}{I_1}\right)\frac{I_3\omega_3^2}{2mgl}$, the condition (28) for the fast top gives:

$$\frac{p_\psi^2}{a} \gg 2\left(\frac{I_3}{I_1}\right) \tag{29a}$$

Therefore, except in the case that $I_3 \ll I_1$ , it holds $\overline{p} \gg \overline{q}$ , and therefore the solution of eq(27m) is approximated by:

$$x_1 = \frac{\overline{q}}{\overline{p}} \tag{29b}$$

Neglecting the term $2\cos\theta_0$ compared to $p_\psi^2 / a$ , Eq(29b) can approximate the *extent* of nutation by the simple formula:

$$u_2 - u_1 \approx \frac{I_1}{I_3}\frac{2mgl}{I_3\omega_3^2}\sin^2\theta_0, \tag{29c}$$

where $\theta_0$ is the initial condition. Thus, the higher the angular velocity $\omega_3$ is the smaller the nutation.

Since the amount of nutation is small, the term $\left(1 - u^2\right)$ in Eq(27i) can be replaced by its initial value, $\sin^2\theta_0$ . By virtue of Eq(29c), and considering the variable transformation $y = x - x_1/2$ for $f(u) = 0$ , Eq(27i) finally becomes:

$$\ddot{y} = -\left(\frac{I_3}{I_1}\omega_3\right) y \tag{29d}$$

From elementary mechanics Eq(29d) dictates that, for the fast top, the frequency of the nutation, in terms of its angular velocity *k*, is given by:

$$k = \frac{I_3}{I_1}\omega_3, \tag{30}$$

and therefore it *increases* the faster the top is spun initially. Based on the calculated extent $\Delta u = u_2 - u_1 = \cos\theta_2 - \cos\theta_1$ , we can determine the extent of the inclination angle $\Delta\theta = \theta_2 - \theta_1$ . Then, the variation of the inclination angle is approximated by:

$$\theta(t) = \theta_1 + \frac{\Delta\theta}{2}(1 - \cos kt). \tag{31}$$

According to French [11, p.694], "if the initial conditions are varied, different types of nutational motion may occur, but they are all understandable in terms of the principles underlying the above analysis".

Due to the nutation, the angular velocity of precession is harmonic of the form:

$$\dot{\phi} = \frac{mgl}{I_3\omega_3}(1 - \cos kt) \tag{32a}$$

of which the amplitude is recognized as the $p_{slow}$ [Eq(25g)]. Although the rate of precession varies harmonically with time, with the same frequency as the nutation, the *average* precession frequency is:

$$\overline{\dot{\phi}} = \frac{mgl}{I_3\omega_3} = p_{slow} \tag{32b}$$

## 4. THREE MAIN ALTERNATIVE FORMULATIONS AND THEIR NUMERICAL INTEGRATION

### 4.1. Based on the totality of dynamic Euler's equations

Since the right-hand side of (3) includes terms in Euler angles, it becomes necessary to solve in these angles (primary variables) instead of the angular velocities. It will be shown that the system of equations takes the standard form

$$\dot{\mathbf{y}} = f\left(t, \mathbf{y}\right), \tag{33}$$

where $\mathbf{y}$ denotes the vector of *five* variables.

Actually, substituting (2) and (6) into (3) we obtain a second-order system of three differential equations in the three Euler angles ( $\phi, \theta, \psi$ ). Although the standard Runge-Kutta procedure would normally lead to six equations of first-order, however, since $M_3 = 0$ and due to the symmetry $\left(I_1 = I_2\right)$, Eq.(3c) implies $\dot{\omega}_3 = 0$ . Therefore, as Eq(2c) suggests, a linear dependency between the rotation about the z-axis and the rest two Euler angles: $\dot{\psi} = \omega_3 - \dot{\phi}\cos\theta$ .

Therefore, by choosing the auxiliary variables as:

$$y_1 = \phi, y_2 = \dot{\phi}, y_3 = \theta, y_4 = \dot{\theta}, y_5 = \psi\ , \tag{34}$$

the final system to be solved becomes:

$$\begin{Bmatrix} \dot{y}_1 \\ \dot{y}_2 \\ \dot{y}_3 \\ \dot{y}_4 \\ \dot{y}_5 \end{Bmatrix} = \begin{Bmatrix} y_2 \\ r_2 \\ y_4 \\ r_4 \\ \omega_3 - y_2\cos y_3 \end{Bmatrix} \tag{35}$$

The functions $r_2$ and $r_4$ that appear in the right-hand side of (35) are derived from the solution of the linear system:

$$\begin{bmatrix} a_{11} & a_{12} \\ a_{21} & a_{22} \end{bmatrix} \cdot \begin{bmatrix} r_2 \\ r_4 \end{bmatrix} = \begin{bmatrix} b_1 \\ b_2 \end{bmatrix} \tag{36}$$

In (36) the four matrix elements are given by:

$$\begin{aligned} a_{11} &= I_1 \sin y_5 \sin y_3 \\ a_{12} &= I_1 \cos y_5 \\ a_{21} &= I_2 \cos y_5 \sin y_3 \\ a_{22} &= -I_2 \sin y_5 \end{aligned} \tag{37}$$

Also, the right-hand sides of (36) are given by:

$$\begin{aligned} b_1 &= mgl \sin y_3 \cos y_5 - a_{13}y_2y_6 - a_{14}y_2y_4 \\ &\quad - a_{15}y_4y_6 - a_{16}y_2 - a_{17}y_4 \\ b_2 &= -mgl \sin y_3 \sin y_5 - a_{23}y_2y_6 - a_{24}y_2y_4 \\ &\quad - a_{25}y_4y_6 - a_{26}y_2 - a_{27}y_4 \end{aligned}, \tag{38}$$

with

$$\begin{aligned} y_6 &= \omega_3 - y_2\cos y_3 \\ a_{13} &= I_1 \cos y_5 \sin y_3 \\ a_{14} &= I_1 \sin y_5 \cos y_3 \\ a_{15} &= -I_1 \sin y_5 \\ a_{16} &= -\omega_3\left(I_2 - I_3\right)\cos y_5 \sin y_3 \\ a_{17} &= \omega_3\left(I_2 - I_3\right)\sin y_5 \end{aligned} \tag{39}$$

and also:

$$\begin{aligned} a_{23} &= -I_2 \sin y_5 \sin y_3 \\ a_{24} &= I_2 \cos y_5 \cos y_3 \\ a_{25} &= -I_2 \cos y_5 \\ a_{26} &= -\omega_3\left(I_3 - I_1\right)\sin y_5 \sin y_3 \\ a_{27} &= -\omega_3\left(I_3 - I_1\right)\cos y_5 \end{aligned} \tag{40}$$

It is noted that in the system (34) the Euler angle $\psi$ is an integral part because it is involved in (37) and (38).

### 4.2. Based on Lagrange's equations

It will be shown that the system of equations takes the standard form $\dot{\mathbf{y}} = f\left(t, \mathbf{y}\right)$, where now $\mathbf{y}$ denotes the vector of *four* variables.

If Eq(15a) is solved in $\dot{\phi}$ it gives:

$$\dot{\phi} = \frac{\left(c_1 - I_3\omega_3\cos\theta\right)}{I_1 \sin^2\theta} \tag{41}$$

Substituting (41) into Eq(14b) one receives:

$$\begin{aligned} \ddot{\theta} &= \left[\frac{\left(c_1 - I_3\omega_3\cos\theta\right)}{I_1\sin^2\theta}\right]^2 \sin\theta\cos\theta \\ &\quad - \left(\frac{I_3\omega_3}{I_1}\right)\left[\frac{\left(c_1 - I_3\omega_3\cos\theta\right)}{I_1\sin^2\theta}\right]\sin\theta + \frac{mgl}{I_1}\sin\theta \end{aligned} \tag{42}$$

As previously, the last equation of the system is:

$$\dot{\psi} = \omega_3 - \dot{\phi}\cos\theta\ , \tag{43}$$

which when combined with (41) gives the following:

$$\dot{\psi} = \omega_3 - \left[\frac{\left(c_1 - I_3\omega_3\cos\theta\right)}{I_1\sin^2\theta}\right]\cos\theta\ , \tag{44}$$

Therefore, the vector of the four variable is chosen as $\mathbf{y}=\left[y_1,y_2,y_3,y_4\right]^T$, where:

$$y_1=\phi,\ \ y_2=\theta,\ \ y_3=\dot{\theta},\ \ y_4=\psi \tag{45}$$

The system $\dot{\mathbf{y}}=f\left(t,\mathbf{y}\right)$ is produced when considering (i) Eq(41) for $\dot{y}_1$, (ii) $\dot{y}_2=y_3$, (iii) Eq(42) for $\dot{y}_3$, and (iv) Eq(44) for $\dot{y}_4$.

**Remarks**

1) Since the Lagrange equations (14) do not directly include the Euler angle $\psi$ (it appears indirectly in 14c), the position of the center of mass and the estimation of the total energy can be found in terms of four variables only, i.e. $\phi,\dot{\phi},\theta,\dot{\theta}$.
2) Since $\dot{\phi}$ is calculated from Eq(41), the conservation of the angular momentum $p_\phi=c_1$ is taken for granted.
3) Equation (42) includes *only* the Euler angle $\theta$, therefore it is an ordinary differential equation of second order that could be separately solved. The numerical integration of the latter could be performed using any known scheme such as Runge-Kutta or Crank-Nicolson algorithms. Afterwards, the calculation of $\dot{\phi}$ through Eq(41) and of $\dot{\psi}$ through Eq(43) or Eq(44) will follow. The integration of $\dot{\phi}$ and $\dot{\psi}$ could be separately performed.

### 4.3. Based on two system invariants

Without details, it has been written in several textbooks that, theoretically, one equation in the system that describes the motion of the spinning top could be replaced by the energy conservation [12,13]. In the same framework, it is well known that in one-dimensional problems the conservation of energy can be used to derive the derivative of the motion variable (displacement or angle) and then analytically integrate the equations [15, p.354 (Wiley-Toppan, 1966)].

In our case, substituting Eq(41) in Eq(18), and then solving in $\dot{\theta}$, one obtains:

$$\dot{\theta}=\pm\left\{\frac{2}{I_1}\left(c_2-\frac{1}{2}I_3\omega_3^2-mgl\cos\theta\right)-\left[\frac{\left(c_1-I_3\omega_3\cos\theta\right)}{I_1\sin\theta}\right]^2\right\}^{1/2} \tag{46}$$

The analytical integration of Eq(46) has been previously obtained using elliptic integrals [1-4]. Under certain circumstances, Eq(46) can be also integrated in a numerical way. One difficulty is that the sign preserves its value only between two successive "turning" points of the nutation provided the initial derivative is different than zero. In particular, when the initial condition is $\dot{\theta}_0=0$, the Runge-Kutta method is not applicable. To make this point clear, without loss of generality, let us consider the simplest forward Euler method (not applied in this paper): $\theta_{n+1}=\theta_n+\Delta t\dot{\theta}\left(t_n,\theta_n\right)$. Since Eq(46) fulfils the initial condition $\dot{\theta}_0=0$, the aforementioned recurrence formula will always vanish ($\theta_1=\theta_2=\ldots=\theta_n=0$). The same conclusion holds for Crank-Nicolson and Runge-Kutta schemes. But even if the initial conditions are different than zero, Eq(46) is applicable only until the next "turning point" at which $\dot{\theta}_{turn}=0$. At the latter point, the numerical solution crashes and always leads to the same stable value (exactly as happen when the initial point was $\dot{\theta}_0=0$).

#### 4.3.1 Scenario 1

Again, the abovementioned scenario of considering a system of *three* equations of first order $\dot{\mathbf{y}}=f\left(t,\mathbf{y}\right)$, i.e. Eq(41) for $\dot{\phi}$, Eq(46) for $\dot{\theta}$, and eq(44) for $\dot{\psi}$, is applicable for only a small period of time (less than one-quarter of the nutation period).

#### 4.3.2 Scenario 2

Alternatively, we propose the use of Eq(42), which is a second order ODE that can be easily solved using either of the Runge-Kutta or Crank-Nicolson methods. For every time step, we accept the calculated value $\theta_{n+1}$ "as is" and then we modify the value of $\dot{\theta}_{n+1}$ according to Eq(46). Then, we perform the next step based on the corrected value of $\theta_{n+1}$, and so on.

In both above scenarios, due to the calculation of $\dot{\phi}$ according to Eq(41), not only the energy ($c_2$) but also the angular momentum ($c_1$) are preserved.

## 5. SUPPORT FORCES

Applying second Newton's law with respect to the Cartesian space system, the three components of the support force at the fixed point (axis origin O) are given by:

$$F_{\text{support},x}=m\ddot{x}_{1,C}, \tag{47a}$$

$$F_{\text{support},y}=m\ddot{y}_{1,C}, \tag{47b}$$

$$F_{\text{support},z}=m\left(g+\ddot{z}_{1,C}\right) \tag{47c}$$

By virtue of Eq(4a), the components of the acceleration at the center of mass C, in the space axes, are given by:

$$\begin{aligned}\ddot{x}_{1,C}=l\big[&\ddot{\phi}\cos\phi\sin\theta+\ddot{\theta}\sin\phi\cos\theta\\&-\left(\dot{\phi}^2+\dot{\theta}^2\right)\sin\phi\sin\theta+2\dot{\phi}\dot{\theta}\cos\phi\cos\theta\big],\end{aligned} \tag{48a}$$

$$\begin{aligned}\ddot{y}_{1,C}=l\big[&\ddot{\phi}\sin\phi\sin\theta-\ddot{\theta}\cos\phi\cos\theta\\&+\left(\dot{\phi}^2+\dot{\theta}^2\right)\cos\phi\sin\theta+2\dot{\phi}\dot{\theta}\sin\phi\cos\theta\big],\end{aligned} \tag{48b}$$

$$\ddot{z}_1=-l\left(\ddot{\theta}\sin\theta+\dot{\theta}^2\cos\theta\right) \tag{48c}$$

In addition, the two components on the horizontal plane can be split in the radial and circumferential direction (with direction cosines $\mathbf{e}_r = \left[\sin\phi \quad -\cos\phi\right]^T$ and $\mathbf{e}_\theta \equiv \mathbf{n}_0 = \left[\cos\phi \quad \sin\phi\right]^T$, respectively) as follows:

$$\begin{Bmatrix} F_{\text{support},r} \\ F_{\text{support},\theta} \end{Bmatrix} = \begin{bmatrix} \sin\phi & -\cos\phi \\ \cos\phi & \sin\phi \end{bmatrix} \begin{Bmatrix} F_{\text{support},x} \\ F_{\text{support},y} \end{Bmatrix} \tag{49}$$

Substituting (47) and (48) into (49), one finally obtains:

$$F_{\text{support},r} = ml\left[\ddot{\theta}\cos\theta - \left(\dot{\phi}^2 + \dot{\theta}^2\right)\sin\theta\right], \tag{50a}$$

$$F_{\text{support},\theta} = ml\left(\ddot{\phi}\sin\theta + 2\dot{\phi}\dot{\theta}\cos\theta\right), \tag{50b}$$

$$F_{\text{support},z} = m\left[g - l\left(\ddot{\theta}\sin\theta + \dot{\theta}^2\cos\theta\right)\right] \tag{50c}$$

Although the derivative of the Euler angle $\psi$ and the relevant component $\omega_3$ influence the numerical solution, it can be noticed that they are not included in the above expressions.

## 6. NUMERICAL RESULTS

The theory will be validated by two numerical examples, the first taken from literature whereas the second is of practical mechanical engineering importance. In addition to ODE45 (MATLAB), in house Runge-Kutta and Crank-Nicolson methods have been used.

The accuracy of the numerical solution has been tested either by the degree of approximating (i) the conservation of energy or (ii) the conservation angular momentum. Since Eq(2c) is the standard one that always participates in the system of equations, it will be completely fulfilled. Moreover, Equations (2a) and (2b) are by-products and there is no apparent measure to evaluate their accuracy. Consequently, two apparent residuals $\left(R_1, R_2\right)$ are those appearing in the first two dynamical Euler equations [(3a) and (3b)], which are given below:

$$R_1 = \left[I_1\dot{\omega}_1 - \left(I_2 - I_3\right)\omega_2\,\omega_3\right] - mgl\sin\theta\cos\psi\,, \tag{51a}$$

$$R_2 = \left[I_2\dot{\omega}_2 - \left(I_3 - I_1\right)\omega_3\,\omega_1\right] + mgl\sin\theta\sin\psi\,, \tag{51b}$$

where

$$\begin{aligned}\dot{\omega}_1 &= \ddot{\phi}\sin\theta\sin\psi + \ddot{\theta}\cos\psi + \dot{\phi}\dot{\theta}\cos\theta\sin\psi \\ &\quad - \dot{\theta}\dot{\psi}\sin\psi + \dot{\psi}\dot{\phi}\sin\theta\cos\psi \\ \dot{\omega}_2 &= \ddot{\phi}\sin\theta\cos\psi - \ddot{\theta}\sin\psi + \dot{\phi}\dot{\theta}\cos\theta\cos\psi \\ &\quad - \dot{\theta}\dot{\psi}\cos\psi - \dot{\psi}\dot{\phi}\sin\theta\sin\psi\end{aligned}$$

Also, the residuals for the violation in the conservation of space $z_1$-momentum ($R_3$) and the conservation of energy ($R_4$) are given by:

$$R_3 = \left[I_1\dot{\phi}\sin^2\theta + I_3\omega_3\cos\theta\right] - c_1\,, \tag{51c}$$

$$R_4 = \left[\frac{1}{2}I_1\left(\dot{\theta}^2 + \dot{\phi}^2\sin^2\theta\right) + \frac{1}{2}I_3\omega_3^2 + mgl\cos\theta\right] - c_2 \tag{51d}$$

### 6.1. Example 1: A slow top

For reasons of comparison, we closely follow the data previously used in literature [30, pp.138-139]. In addition, we also present many comments related to the mechanics involved and the auxiliary use of the available closed form analytical solutions.

It is reminded that in matrix form (see Appendix A), the relationship between the transformation matrix **A** and the matrix of angular velocities $\boldsymbol{\Omega}$ is as follows:

$$\dot{\mathbf{A}}^T = \mathbf{A}^T \cdot \boldsymbol{\Omega}, \quad \text{where} \quad \boldsymbol{\Omega} = \begin{bmatrix} 0 & -\omega_3 & \omega_2 \\ \omega_3 & 0 & -\omega_1 \\ -\omega_2 & \omega_1 & 0 \end{bmatrix}$$

The matrix **A** includes only the Euler angles whereas the angular velocity includes their derivatives. Therefore, the initial conditions must include data from both matrices. In more detail, the initial data where $\phi_0 = 0, \dot{\phi}_0 = 0$, $\theta_0 = \pi/16, \dot{\theta}_0 = 0$, and $\psi_0 = \pi/16, \dot{\psi}_0 = 1$, whence

$$\mathbf{A}_0 = \begin{bmatrix} 1.0 & 0.0 & 0.0 \\ 0.0 & \cos\left(\phi_0\right) & \sin\left(\phi_0\right) \\ 0.0 & -\sin\left(\phi_0\right) & \cos\left(\phi_0\right) \end{bmatrix} \text{ and}$$

$$\boldsymbol{\Omega}_0 = \begin{bmatrix} 0 & -\omega_{3,0} & \omega_{2,0} \\ \omega_{3,0} & 0 & -\omega_{1,0} \\ -\omega_{2,0} & \omega_{1,0} & 0 \end{bmatrix} = \begin{bmatrix} 0.0 & -1.0 & 0.0 \\ 1.0 & 0.0 & 0.0 \\ 0.0 & 0.0 & 0.0 \end{bmatrix},$$

Following [30], the inertia tensor **J**, the center of mass $\mathbf{r}_C$ with respect to the body system were given as

$$\mathbf{J} = \begin{bmatrix} I_1 & 0 & 0 \\ 0 & I_2 & 0 \\ 0 & 0 & I_3 \end{bmatrix} = \frac{1}{8}\begin{bmatrix} 7 & 0 & 0 \\ 0 & 7 & 0 \\ 0 & 0 & 2 \end{bmatrix} \text{ (kg.m}^2\text{)}, \quad \mathbf{r}_C = \begin{bmatrix} 0 \\ 0 \\ l \end{bmatrix},$$

with $l = \sqrt{3}/2$ m.

Moreover, with respect to the space (global) system, the vector of the external torque is taken to be produced by the weight *m*g of the spinning top at the center of mass C, which for the fixed (space) system is:

$$m\mathbf{g} = m\begin{bmatrix} 0 \\ 0 \\ -9.81 \end{bmatrix} \text{ (m.s}^{-2}\text{), with } m = 1 \text{ kg.}$$

As was previously mentioned, the right-hand side of dynamic Euler's equations (3) is given by Eq (6), which considers the projection of the vector representing the external torque onto the body axes.

This case appears a much extended nutation. The numerical results are valid only if the top is mechanically supported by a stand that allows it to dip below the horizontal level. In more details, the topology of the stand must be so that it is capable of exerting either compressive (above the horizontal) or tensile (below the horizontal) support forces. The latter (below the horizontal) is crucial because otherwise the top will detach from its support point.

### 6.1.1 Analytical calculations

A first observation is that the major initial condition $\theta_0 = \pi/16, \dot{\theta}_0 = 0$ is concerned with instantaneous stillness of the body $z$ axis, which is equivalent with a turning point of nutation ($u_1 = \pi/16$). The immediately next turning point is accurately calculated by Eq(27g), which provides two feasible solutions, i.e. $u_1 \approx 0.9808$ (corresponds to 11.25 degrees, being the initial angle $\theta_0 = \pi/16$) and $u_2 \approx$-0.9958 (corresponds to $\theta_{turn} = 174.8$ degrees). Therefore, it is anticipated that the spinning top will perform large scale nutation in the interval $\theta \in [11.25, 174.8]$ degrees.

Concerning the angular velocity of precession, it varies between zero (at $\theta_0 = 11.25$ deg) and a maximum value $\dot{\phi}_{\max} =$ 67.97 rad/s (appearing at the lowest position $\theta_{turn} = 174.8$ deg). It is noted that if we try to take the first derivative of $\dot{\phi}$ in Eq(41) and equalize to zero, it leads to a quadratic polynomial with negative determinant, a fact that proves that $\ddot{\phi}$ is permanently positive until the lowest point thus no other local maximum exists in between $\theta_0 = 11.25$ and $\theta_{turn} = 174.8$ deg.

It is also noted that in this example, since $1/2\, I_3 \omega_3^2 = 0.125 << 2mgl = 19.62$, Eq(27m) must be applied and taking the positive sign we obtain $x_1 \approx 1.967$, which corresponds to 84.8 degrees below the horizontal, a fact verified with the numerical solution presented below. As it will be validated in the next Section, the set of simple formulas from Eq(29c) to Eq(32b) induce tremendous error and therefore are not applicable.

### 6.1.2 Numerical computations

In the sequence we present the numerical solution obtained using several schemes: Euler [Eq(35)], Lagrange [Eq(45)] and two energy conservation schemes. In order to avoid the use of elliptical integrals, as an "exact" solution we have taken the ODE45 MATLAB solution using an extremely small tolerance of order $10^{-14}$. For a better evaluation, we present the response for three cycles of precession ( $\Delta\theta = 3\times360$ degrees of azimuthal angle), which here corresponds to almost three cycles of nutation. For the data of this example, the invariants of the mechanical systems are $c_1 \cong 0.245$ and $c_2 \cong 8.46$.

In Euler formulation (Section 4.1), the first two residuals ($R_1$ and $R_2$ in Eq(51)) are zero whereas the last two ($R_3$ and $R_4$) vary in time (**Figure 2**). It can be noticed that the period is about 2.22 seconds. MATLAB ODE45 was applied using the default accuracy.

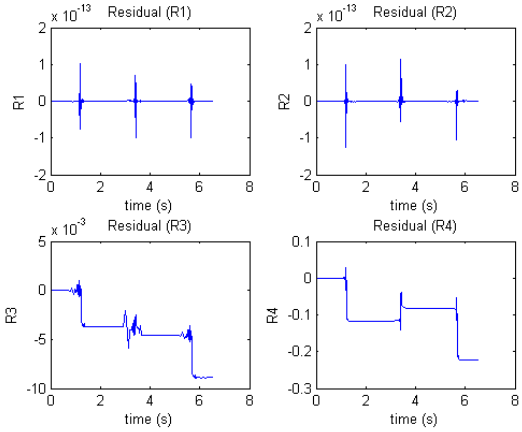


**Figure 2.** Calculated residuals ($R_1, R_2, R_3, R_4$) based on Eq(51), using ODE45 for the Euler formulation (336 unequal steps).

In Lagrange formulation (Section 4.2), as previously, the first two residuals are zero. In addition, no variation of $c_1$ was observed ($R_3$=0). Moreover, not only the energy is not preserved ($R_4 \neq 0$) but it also appears singularities when the center of mass passes through the horizontal. Concerning the angular momentum, both $R_1$ and $R_2$ vary in time (**Figure 3**). MATLAB ODE45 was applied using the default accuracy.

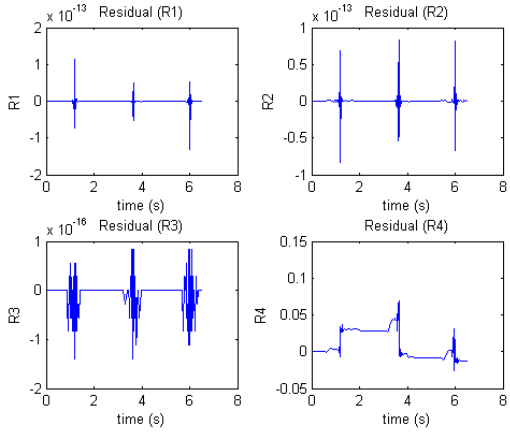


**Figure 3.** Calculated residuals ($R_1, R_2, R_3, R_4$) based on Eq(51), using ODE45 for the Lagrange formulation (248 unequal steps).

In house standard RK2 and RK4 Runge-Kutta algorithms using a constant step (Appendix C) during the whole procedure leads to extremely high singularities ($R_1$ and $R_2$ of the order $10^{-10}$, whereas $R_4$ of the order $10^9$) when using the same number of time steps with the ODE45 (248 steps). However, when the number of steps was increased by a factor of four, i.e. from 248 to 992, then the time response using RK4 becomes more reasonable as shown in **Figure 4**. Concerning RK2,

similar accuracy is obtained when the number of steps increases by a factor of 16 to 3968 (= 16×248 = 4×992).

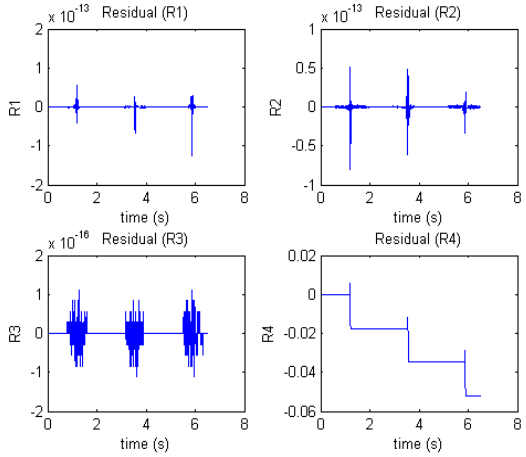


**Figure 4.** Calculated residuals $(R_1, R_2, R_3, R_4)$ based on Eq(51), using RK4 (992 equal steps) for the Lagrange.

Also, the Crank-Nicolson method (Appendix D) based on two slightly different schemes leads to similar results than the RK4 scheme for the same number of time steps. For both schemes (Scheme-1 and Scheme-2), the minimum multiple of 248 to obtain acceptable results is 4×248=992 steps (very similar to RK4). The results are shown in **Figure 5** and **Figure 6** for scheme-1 and scheme-2, respectively.

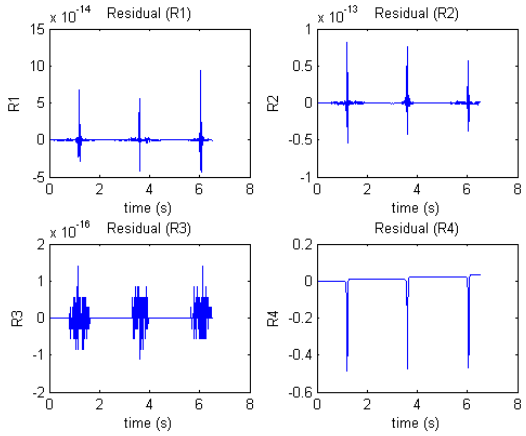


**Figure 5.** Calculated residuals $(R_1, R_2, R_3, R_4)$ based on Eq(51), using Crank-Nicolson Scheme-1 for the Lagrange formulation (992 equal steps).

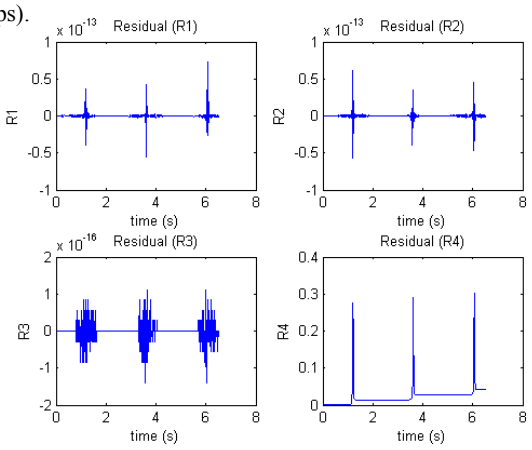


**Figure 6.** Calculated residuals $(R_1, R_2, R_3, R_4)$ based on Eq(51), using Crank-Nicolson Scheme-2 for the Lagrange formulation (992 equal steps).

In the sequence, in order to include the constraint of constant total energy, we apply the two scenarios mentioned in Section 4.3. The results are as follows.

**Scenario-1**: As an initial state we considered the numerical solution at the time $t = T_n/8$ ($T_n$ = nutation period), as obtained using the ODE45 MATLAB implementation of the Lagrange formulation for very small tolerance (RelTol=1e-14, AbsTol=1e-14). It is noted that all four residuals were of the order $10^{-14}$ but numerical solution crashed after $T_n/8$ at the first turning point.

**Scenario-2**: Now the initial conditions were taken again equal to $\phi_0 = 0, \dot{\phi}_0 = 0$, $\theta_0 = \pi/16, \dot{\theta}_0 = 0$, and $\psi_0 = \pi/16, \dot{\psi}_0 = 1$. For a better control of the computer program, the latter was developed in conjunction with the in house RK4. No problem was noticed and all residuals were found at the limit of computer accuracy as shown in **Figure 7**.

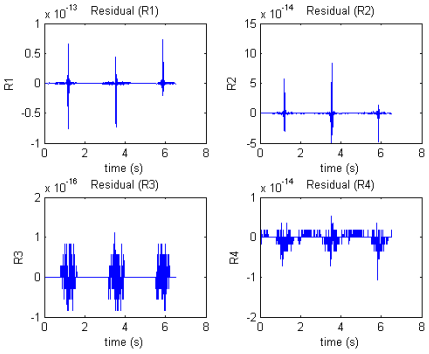


**Figure 7.** Calculated residuals $(R_1, R_2, R_3, R_4)$ based on Eq(51), using RK4 (992 equal steps) for the Lagrange formulation (Scenario-2: Eq(42)) in conjunction with a-posteriori correction for energy conservation using Eq(46).

The time history for the three Euler angles $\phi, \theta, \psi$ as well as for the level $z_c$ of the center of mass is shown in the typical **Figure 8**; no visually significant differences were noticed for all models. It is worth-mentioning that the numerical solution predicts the extreme (turning) point at 174.8, which is identical to the aforementioned analytical value mentioned in Section 6.1.1 [Eq(27g) or Eq(27m)]. It is again noted that Eq(29c) is not applicable.

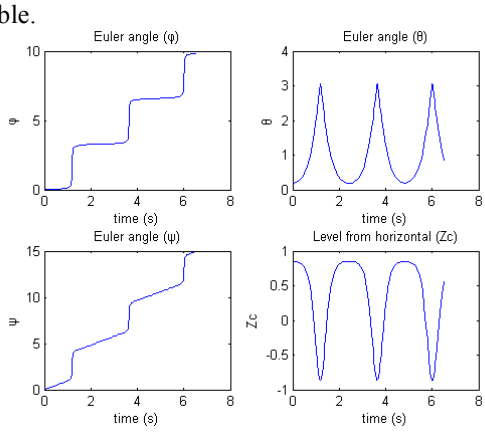

**Figure 8.** Euler angles and distance of the center of mass from the horizontal using ODE45 MATLAB solution with 248 steps of variable size.

Moreover, the time history of the components of the support forces are shown in **Figure 9** where one can notice that the vertical is initially upward (positive) until the body $z$ axis reaches the horizontal and then it becomes downward (negative) until the lowest turning point. In the bottom right of the same figure, we also include the total energy and its distribution in terms of potential and kinetic components.

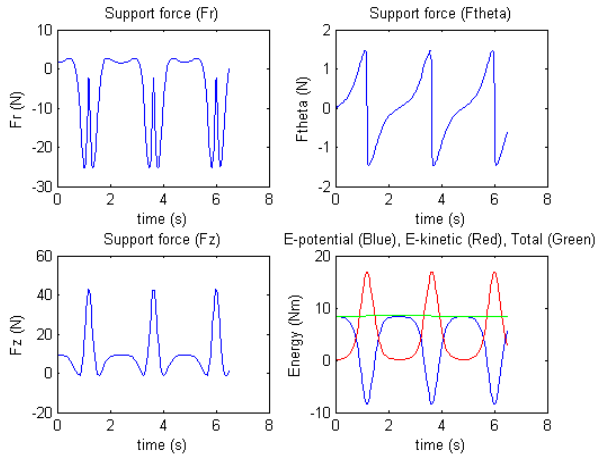


**Figure 9.** Support forces and energy using ODE45 MATLAB solution with 248 steps of variable size.

As previously mentioned, the difference between the analytical [Eq(29c) until Eq(32b)] and the numerical solution was found to be enormous. In other words, the aforementioned analytical solutions are not applicable to a slow top as the case of this example.

## 6.2 Example 2: The spinning wheel

The meaning of this example is that it offers the possibility to modify parameters in the real world. It refers to a spinning flywheel, which is mounted at the end of a massless rigid rod of length $l$ as shown in **Figure 10**. The flywheel is a cylindrical body of radius $r$ and thickness $h$. The rigid rod is connected at the center of mass of the aforementioned cylindrical body. Under these circumstances, the momenta of inertia with respect to the origin O are given by:

$$I_1 = \frac{m}{12}\left(3r^2 + h^2\right) + ml^2, \quad I_3 = \frac{m}{2}r^2 \qquad (52)$$

We choose the following data:
Length of rod: $l = 1.0$ m
Gravitational acceleration: $g = 9.81$ m/sec$^2$
Thickness of spinning wheel: $h = 0.010$ m
Density: $\rho = 7800$ kg/m$^3$
Radius of spinning wheel: $r = 0.10$m (see Fig.10)
Mass of wheel: $m = \rho\, h\, \pi\, r^2$ ($\cong 2.45$ kg)

Initial conditions: $\phi_0 = 0, \dot{\phi}_0 = 0$ , $\theta_0 = \pi/16, \dot{\theta}_0 = 0$ , and $\psi_0 = 0, \dot{\psi}_0 = \text{variable}$.

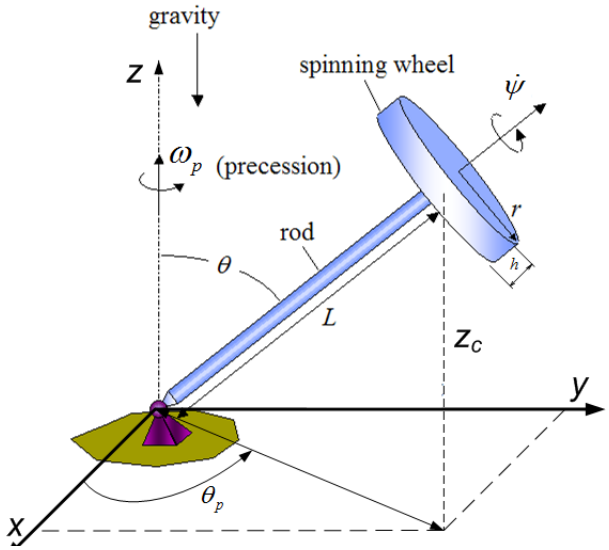


**Figure 10.** Spinning wheel.

According to Eq(28), the characterization of a "fast top" occurs when $I_3\omega_3^2 >> 4mgl$, or equivalently [by virtue of (52)]. Therefore:

Condition for fast top: $\omega_3^2 >> 8gl/r^2$. (53)

For the particular data, the critical angular velocity of the spinning wheel equals to $\omega_{3,CR}^2 = 7848$ s$^{-2}$ (therefore $\omega_3 >> \omega_{3,CR} = 88.6$ s$^{-1}$ $\cong$ 846 RPM).

In order to validate the analytical solutions, numerical solutions are derived for several multiples and submultiples of the critical angular velocity $\omega_{3,CR}$ ($\omega_3 = \lambda\omega_{3,CR}$, $0.1 \le \lambda \le 10$) using ODE45 MATLAB (for the default) in conjunction with Lagrange formulation (Section 4.2). **Table 1** presents the comparison of results obtained using analytical and numerical solution. Therefore, if the average angular velocity $\overline{\dot{\phi}}$ is estimated by Eq(32b), the calculated period does not always correspond to azimuthal angle of 360 degrees. For example, one can notice in Table 1 that at the critical condition ($\omega_3 = \omega_{3,CR}$) it corresponds to 428.1 degrees, at a double value to 373.1 degrees, whereas at a half value to 338.2 degrees. It can be also noticed that when the spin velocity is smaller than $\omega_{3,CR}/2$ the center of mass may travel below the horizontal level, whereas when $\omega_3 > \omega_{3,CR}$ the nutation is small and for still higher spins it tends to vanish.

**Table 1**: Evaluation of analytical solutions

| Multiple or sub-multiple of $\omega_{3,CR}$ ($\lambda$) | Angular velocity ($\omega_3$) | | Maximum angle ($\phi$) in degrees, based on (32b) | Minimum Level $Z_{C,min}$ | Maximum Level $Z_{C,max}$ |
|---|---|---|---|---|---|
| | ($s^{-1}$) | (RPM) | | | |
| 0.1 | 8.86 | 84.6 | 6.9 | -0.9606 | 0.9808 |
| 0.2 | 17.72 | 169.2 | 76.9 | -0.8425 | 0.9808 |
| 0.3 | 26.58 | 253.8 | 229.5 | -0.6450 | 0.9808 |
| 0.4 | 35.44 | 338.4 | 293.5 | -0.3692 | 0.9808 |
| 0.5 | 44.29 | 423.0 | 338.2 | -0.0224 | 0.9808 |
| 0.6 | 53.15 | 507.6 | 410.0 | 0.3899 | 0.9808 |
| 0.7 | 62.01 | 592.2 | 503.8 | 0.7822 | 0.9808 |
| 0.8 | 70.87 | 676.8 | 484.3 | 0.9220 | 0.9808 |
| 0.9 | 79.73 | 761.4 | 428.8 | 0.9513 | 0.9808 |
| 1.0 | 88.59 | 846.0 | 428.1 | 0.9621 | 0.9808 |
| 1.1 | 97.45 | 930.6 | 404.1 | 0.9675 | 0.9808 |
| 1.5 | 132.88 | 1268.9 | 384.8 | 0.9755 | 0.9808 |
| 2.0 | 177.18 | 1691.9 | 373.1 | 0.9781 | 0.9808 |
| 3.0 | 265.77 | 2537.9 | 365.8 | 0.9797 | 0.9808 |
| 4.0 | 354.36 | 3383.8 | 363.1 | 0.9802 | 0.9808 |
| 5.0 | 442.94 | 4229.8 | 361.6 | 0.9804 | 0.9808 |
| 6.0 | 531.53 | 5075.8 | 361.1 | 0.9805 | 0.9808 |
| 10.0 | 885.89 | 8459.6 | 360.5 | 0.9807 | 0.9808 |
| 20.0 | 1771.78 | 16919.2 | 360.1 | 0.9808 | 0.9808 |

Eq(29c) up to Eq(32b). Basically, there are four physical quantities to calculate:

1) The change $\Delta\theta$ of the inclination angle $\theta$ during nutation. Equivalently, the range in which the $z$-coordinate of the centroid varies. To this, Eq(29c) is applied.
2) The frequency $k$ of the nutation (Eq(30)).
3) The average frequency (equivalently, of angular velocity) of the precession (Eq(32b)).
4) The average number of nutations in a whole period of precession (360 degrees of $\phi$). The latter equals to the ratio of the average frequency of precession over the frequency of nutation. Therefore, by virtue of Eq(30) and Eq(32b), the number of nutations in a whole period of precession are approximated by:

Number of nutations per period of precession:

$$N_{nutations} = \frac{\left(I_3\omega_3\right)^2}{I_1 mgl} \tag{54}$$

For example, in case of $\lambda$=2, Eq(29) gives $u_2 - u_1 \approx 0.0024$, which is very near to the value 0.0027 that was calculated by the ODE45. Also, Eq(54) predicts 31.9 nutations (30.8 when using the correcting factor 360/373.1 according to Table 1), which is very close to the measured 29 nutations as shown in **Figure 11**. It is noted than calculations concern 373.1 degrees of precession, whereas the overlapping of one period of nutation can be noticed near the initial point which is located at $\left(x_0, y_0, z_0\right) \approx \left(0, -0.195, 0.981\right)$.

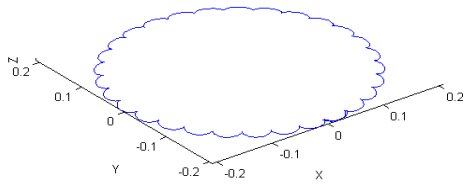


**Figure 11.** Calculated nutations when the initial spin angular velocity is twice larger than the critical value of 88.59 $s^{-1}$.

## 7. DISCUSSION

This study focuses on the "spinning top", which works equivalently with a flywheel at the end of a rigid rod. The common feature is that in both cases the distance of the centroid from the support is different than zero ($l \neq 0$). Although in engineering praxis the so-called "gyroscope" is of higher importance, the only essential difference between a spinning top and a gyroscope lies on the fact that a gyroscope is usually supported at its centroid (thus $l = 0$).

It was shown that, in principle, the ODE45 MATLAB function can be safely applied for the numerical integration of the differential equations of motion, in all formulations. The advantage of this function is that it continuously varies the time step so as to locally achieve the given tolerance.

In general, basic conclusions can be derived on the basis of simple closed form analytical solutions provided we carefully deal with the slow top and fearless with a fast top in which the initial spin is higher than its critical value. In the case of a spinning flywheel of cylindrical shape, a simple formula was given for the aforementioned critical value in Eq(53). It can be noticed than in the latter case the critical spin depends only on the length $l$ and the radius $r$ and not on the thickness $h$ of the cylindrical wheel.

## 8. CONCLUSIONS

In this study we successfully applied several numerical schemes for the solution of the equations of motion for a symmetrical spinning top, which was considered as a rigid body with a fixed and frictionless point. It was found that using the standard MATLAB ODE45 with default accuracy, the Lagrange based formulation requires a smaller number of time steps than the Euler equations formulation (about 36 percent reduction). It was also found that the same occurs when increasing the tolerance variables. Both of the tested Crank-Nicolson schemes did not perform better than in house Runge-Kutta RK4 when applied in conjunction with an invariable size of the time step. Although the ordinary differential equation produced by the energy conservation is solvable in terms of the inclination Euler angle, it was found to be trapped between two "turning points". In contrast, the accuracy was significantly increased when the Lagrange solution was combined with a-posteriori correction of the time

derivative of the inclination angle for each time step. It was clearly shown that although some analytical solutions can be applied to both slow and fast tops, the behavior of fast spinning tops is predicted by much simpler formulas.

## REFERENCES


[1] J. L. Lagrange, Mécanique Analytique, Courcier, Paris (1811)

[2] F. Klein and A. Sommerfeld, The Theory of the Top, Volume 1: Introduction to the Kinematics and Kinetics of the Top, Birkhäuser, Boston (2008); translated by R J Nagen and G Sandri (Originally published 1897 by Teubner)

[3] F. Klein and A. Sommerfeld, The Theory of the Top, Volume 2: Development of the Theory in the Case of the Heavy Symmetric Top, Birkhäuser, Boston (2010); translated by R J Nagen and G Sandri (Originally published 1898 by Teubner)

[4] F. Klein, The Mathematical Theory of the Top, Charles Scribners Sons, New York (1897). Republished in 2004 (Dover, Mineola).

[5] G.G. Appel'rot, The problem of motion of a rigid body about a fixed point, *Uchenye Zap. Mosk.Univ. Otdel.Fiz. Mat. Nauk*, 11, 1-112 (1894)

[6] H. Crabtree, An Elementary Treatment of the Theory of Spinning Tops and Gyroscopic Motion, Longmans-Green-and Co, New York (1909)

[7] John Perry, Spinning Tops, E. S. Gorham, New York (1910). Also: "Spinning Tops and Gyroscopic Motion," Dover Publications, New York (1957)

[8] D.W. Gould, The Top: Universal Toy Enduring Pastime, Bailey Brothers and Swinfen Ltd, Folkestone, UK (1975)

[9] E. T. Whittaker, A Treatise on the Analytical Dynamics of Particles and Rigid Bodies, Dover, New York (1944)

[10] S. J. Zaroodny, An Elementary Introduction to Elliptic Functions Based on the Theory of Nutation, The American Mathematical Monthly, 68(7), 593–616 (1961)

[11] A. P. French, Newtonian Mechanics: The M.I.T. Introductory Physics Series, W. W. Norton & Company Inc., New York (1971)

[12] H. Goldstein, C. Poole and J. Safko, Classical Mechanics, 3rd edition, Pearson Education Inc. (Addison Wesley), San Francisco (2002)

[13] S. Targ, Theoretical Mechanics: A Short Course, Mir Publishers, Moscow, 3rd edition (1976)

[14] V. I. Arnold, Mathematical Methods of Classical Mechanics, vol. 60, Springer-Verlag, New York-Heidelberg-Berlin (1984)

[15] David Halliday, Robert Resnick and Jearle Walker, Fundamental of Physics, 9th edition, John Wiley & Sons, NJ (2011), pp. 294-295.

[16] H. D. Young and R. A. Freedman, University Physics, 12th edition, Pearson Addison-Wesley, San Francisco (2008), pp. 337-340.

[17] Michèle Audin, Spinning Tops: A Course on Integrable Systems, Studies in Advanced Mathematics, Vol. 51, Cambridge University Press, Cambridge (1996)

[18] V. V. Golubev, Lectures on integration of the equations of motion of a rigid body about a fixed point, Gostenhizdat, Moscow, 1953 [in Russian]; English translation: Philadelphia: Coronet Books (1953)

[19] R.H. Cushman and L.M. Bates, Global Aspects of Classical Integrable Systems, Birkhäuser Verlag, Basel, 1997 (Chapter III: The Euler Top, pp. 83-146).

[20] Saul Gorn, The Automatic Analysis and Control of Computing Errors, Journal of the Society for Industrial and Applied Mathematics, SIAM, 2(2), 69–81 (1954)

[21] D.J. McGill and L. S. Long, III, Stability regions for an unsymmetrical rigid body spinning about an axis through a fixed point, Acta Mechanica 22, 91–112 (1975)

[22] J.C. Simo and K.K. Wong, "Unconditionally stable algorithms for rigid body dynamics that exactly preserve energy and momentum," Int. J. Numer. Meth. Engng 31 (1991), 19-52.

[23] J.C. Simo, N. Tarnow and K.K. Wong, Exact energy-momentum conserving algorithms and symplectic schemes for nonlinear dynamics, Comp. Meth. Appl. Mech. Engng 100, 63-116 (1992)

[24] T. Ratiu and P. van Moerbeke, The Lagrange rigid body notion, Ann. Inst. Fourier, Grenoble, 32 (1), 211–234 (1982)

[25] M. Romano, Exact analytic solutions for the rotation of an axially symmetric rigid body subjected to a constant torque, Celest. Mech. Dyn. Astr. 101, 375–390 (2008)

[26] Z. Jackiewicz, A. Marthinsen and B. Owren, Construction of Runge–Kutta methods of Crouch–Grossman type of high order, Advances in Computational Mathematics 13, 405–415 (2000)

[27] K. Engø and A. Marthinsen, A Note on the Numerical Solution of the Heavy Top Equations, Multibody System Dynamics 5, 387–397 (2001)

[28] N.M. Bou-Rabee, J.E. Marsden and L.A. Romero, Tippe Top Inversion as a Dissipation-Induced Instability, SIAM J. Applied Dynamical Systems, 3(3), 352–377 (2004)

[29] R. Kozlov, High-order conservative discretizations for some cases of the rigid body motion, Physics Letters A, 373, 23–29 (2008)

[30] B. Owren and A.Marthiinsen, Runge-Kutta methods adapted to manifolds and based on rigid frames, BIT, 39(1), 116–142 (1999) (particularly pp. 137-140).

[31] A.C. Or, The dynamics of a Tippe Top, SIAM Journal of Applied Mathematics, 54(3), 597–609 (1994)

[32] M.V. Berry and P. Shukla, Slow manifold and Hannay angle in the spinning top, Eur. J. Phys., 32, 115–127 (2011)

[33] G.E. Hay, Vector and Tensor Analysis, Dover Publications, New York (1953), Chapter 3.

[34] S.Kowalevski, Sur le problème de la rotation d'un corps solide autour d'un point fixe, Acta Mathematica, 12 (1889).

[35] R. Cooke, The mathematics of Sonya Kovalevskaya, Springer-Verlag, New York (1984)

[36] S.Kowalevski, Sur une propriété du système d'équations différentielles qui définit la rotation d'un corps solide autour d'un point fixe, Acta Mathematica, 14 (1889).

[37] A.Goriely, M.Nizette, Kovalevskaya rods and Kovalevskaya waves, Regular and Chaotic Dynamics, 5(1), 95–106 (2000)

## APPENDIX A

### Derivation of motion Euler equations using matrices

In general, the relation between the co-ordinates of a vector **v** in the local (body) $Oxyz$ system and the global (space) $Ox_1y_1z_1$ system, is given by the simple formula:

$$\mathbf{v}_{local} = \mathbf{A} \cdot \mathbf{v}_{global}, \tag{A-1}$$

where **A** is the transformation matrix from the space (global) to the body (local) system. In our case, the matrix **A** is given by Eq(5).

Equivalently, it holds:

$$\mathbf{v}_{global} = \mathbf{A}^T \cdot \mathbf{v}_{local}, \tag{A-2}$$

where $\mathbf{A}^T$ is the transpose of the matrix A (obviously, $\mathbf{A}\mathbf{A}^T = \mathbf{A}\mathbf{A}^{-1} = \mathbf{I}$).

The local Cartesian system may be considered that is produced by the global through a rotation $\boldsymbol{\theta} = \mathbf{i}_\theta \theta$ around the unit vector $\mathbf{i}_\theta$. Since the rotation vector $\boldsymbol{\theta}$ can be a function of time, i.e. $\boldsymbol{\theta} = \boldsymbol{\theta}(t)$, then the angular velocity $\boldsymbol{\omega}$ of the rigid body (local system) will be:

$$\boldsymbol{\omega} = \frac{d\boldsymbol{\theta}}{dt} = \begin{bmatrix} \omega_x \\ \omega_y \\ \omega_z \end{bmatrix} \tag{A-3}$$

If we redefine the abovementioned angular velocity in a tensor from:

$$\boldsymbol{\Omega}_{local} = \begin{pmatrix} 0 & -\omega_z & \omega_y \\ \omega_z & 0 & -\omega_x \\ -\omega_y & \omega_x & 0 \end{pmatrix}, \tag{A-4}$$

it can be easily proved that

$$\dot{\mathbf{A}} = \boldsymbol{\Omega}_{local}^T \cdot \mathbf{A}, \text{ or equivalently, } \left(\dot{\mathbf{A}}\right)^T = \mathbf{A}^T \cdot \boldsymbol{\Omega}_{local} \tag{A-5}$$

It is worth-mentioning that the definition of the matrix $\boldsymbol{\Omega}$ in (A-4) has been chosen so as it fulfills the identity: $\boldsymbol{\Omega} \cdot \mathbf{v} = \vec{\boldsymbol{\omega}} \times \vec{\mathbf{v}}$ (matrix product equals to the cross product).

Therefore, the components of the time derivative of the vector **v** are related by:

$$\dot{\mathbf{v}}_{local} = \left(\mathbf{A} \cdot \mathbf{v}_{global}\right)^{\cdot} = \dot{\mathbf{A}}\mathbf{v}_{global} + \mathbf{A} \cdot \dot{\mathbf{v}}_{global}. \tag{A-6}$$

and

$$\dot{\mathbf{v}}_{global} = \left(\mathbf{A}^T \cdot \mathbf{v}_{local}\right)^{\cdot} = \left(\mathbf{A}^T\right)^{\cdot} \mathbf{v}_{local} + \mathbf{A}^T \dot{\mathbf{v}}_{local}, \tag{A-7}$$

By virtue of (A-5), Eq(A-7) becomes;

$$\dot{\mathbf{v}}_{global} = \mathbf{A}^T \cdot \boldsymbol{\Omega}_{local} \cdot \mathbf{v}_{local} + \mathbf{A}^T \dot{\mathbf{v}}_{local}, \tag{A-8}$$

Let us now designate by **L** the angular momentum of the rigid body and M the external moment (or torque). The second Newton's law for the rotation is written as follows:

$$\mathbf{M}_{global} = \frac{d\mathbf{L}_{global}}{dt} \equiv \dot{\mathbf{L}}_{global} \tag{A-9}$$

Since both **M** and **L** are vectors, they obey the general transformation which is given by Eq(A-1) and (A-6). Therefore it holds:

$$\mathbf{M}_{global} = \mathbf{A}^T \cdot \mathbf{M}_{local}, \tag{A-10}$$

$$\mathbf{L}_{global} = \mathbf{A}^T \cdot \mathbf{L}_{local}, \tag{A-11}$$

Substituting (A-10) and (A-11) into (A-9), and considering the identity (A-7), one obtains:

$$\mathbf{A}^T \cdot \mathbf{M}_{local} = \left(\mathbf{A}^T\right)^{\cdot} L_{local} + \mathbf{A}^T \dot{\mathbf{L}}_{local} \tag{A-12}$$

Substituting (A-5) into (A-12) one obtains:

$$\mathbf{A}^T \cdot \mathbf{M}_{local} = \mathbf{A}^T \cdot \boldsymbol{\Omega}_{local} \cdot \mathbf{L}_{local} + \mathbf{A}^T \cdot \dot{\mathbf{L}}_{local} \tag{A-13}$$

Left-multiplying (A-13) by $\mathbf{A}$, considering that $\mathbf{A}\mathbf{A}^T = \mathbf{I}$, and rearranging the left and right members, we receive:

$$\dot{\mathbf{L}}_{local} + \boldsymbol{\Omega}_{local} \cdot \mathbf{L}_{local} = \mathbf{M}_{local} \tag{A-14}$$

Considering the notation appearing in the main text, i.e.:

$$\mathbf{L} = \begin{bmatrix} I_1\omega_1 \\ I_2\omega_2 \\ I_3\omega_3 \end{bmatrix}, \text{ and } \dot{\mathbf{L}} = \begin{bmatrix} I_1\dot{\omega}_1 \\ I_2\dot{\omega}_2 \\ I_3\dot{\omega}_3 \end{bmatrix} \tag{A-15}$$

$$\boldsymbol{\Omega}_{local} = \begin{pmatrix} 0 & -\omega_3 & \omega_2 \\ \omega_3 & 0 & -\omega_1 \\ -\omega_2 & \omega_1 & 0 \end{pmatrix}, \tag{A-16}$$

and

$$\mathbf{M}_{local} = \begin{bmatrix} M_1 \\ M_2 \\ M_3 \end{bmatrix}, \tag{A-17}$$

Equation (A-14) finally becomes:

$$\begin{bmatrix} I_1\dot{\omega}_1 \\ I_2\dot{\omega}_2 \\ I_3\dot{\omega}_3 \end{bmatrix} + \begin{pmatrix} 0 & -\omega_3 & \omega_2 \\ \omega_3 & 0 & -\omega_1 \\ -\omega_2 & \omega_1 & 0 \end{pmatrix} \cdot \begin{bmatrix} I_1\omega_1 \\ I_2\omega_2 \\ I_3\omega_3 \end{bmatrix} = \begin{bmatrix} M_1 \\ M_2 \\ M_3 \end{bmatrix} \tag{A-18}$$

Equation (A-18) is identical with Eq(3a,b,c), and this completes the proof.

## APPENDIX B

### The angular velocity in the fixed co-ordinate system

Applying (A-2) for the vector $\mathbf{v}_{local} = \begin{bmatrix} \omega_1 & \omega_2 & \omega_3 \end{bmatrix}^T$, of which the components in the fixed system is $\mathbf{v}_{global} = \begin{bmatrix} \omega_{x1} & \omega_{y1} & \omega_{z1} \end{bmatrix}^T$, we finally obtain:

$$\begin{aligned} \omega_{x1} &= \dot{\theta}\cos\phi + \dot{\psi}\sin\phi\sin\theta, \\ \omega_{y1} &= \dot{\theta}\sin\phi - \dot{\psi}\cos\phi\sin\theta, \\ \omega_{z1} &= \dot{\phi} + \dot{\psi}\cos\theta. \end{aligned} \tag{B-1}$$

It is remarkable that the same result will be obtained if we transform the tensor $\mathbf{\Omega}_{local}$ given in (A-16) to the $\mathbf{\Omega}_{global}$, using the formula:

$$\mathbf{\Omega}_{global} = \mathbf{A}^T \mathbf{\Omega}_{global} \mathbf{A} \tag{B-2}$$

## APPENDIX C
### Runge-Kutta algorithms as applied

For a first order differential system

$$\dot{\mathbf{y}} = \dot{\mathbf{f}}\left(t, \mathbf{y}\right), \tag{C-1}$$

with initial conditions

$$\mathbf{y}\left(0\right) = \mathbf{y}_0, \tag{C-2}$$

the *two-point* Runge-Kutta (RK2) solution is produced using the recursion:

$$\begin{aligned} \mathbf{y}_{n+1} &= \mathbf{y}_n + \mathbf{k}_2 + \mathrm{O}\left(h^3\right) \\ \mathbf{k}_1 &= h\dot{\mathbf{f}}\left(t_n, \mathbf{y}_n\right), \\ \mathbf{k}_2 &= h\dot{\mathbf{f}}\left(t_n + \frac{h}{2}, \mathbf{y}_n + \frac{\mathbf{k}_1}{2}\right) \end{aligned} \tag{C-3}$$

Also, the *four-point* Runge-Kutta (RK4) solution is produced using the recursion:

$$\begin{aligned} \mathbf{y}_{n+1} &= \mathbf{y}_n + \frac{\mathbf{k}_1}{6} + \frac{\mathbf{k}_2}{3} + \frac{\mathbf{k}_3}{3} + \frac{\mathbf{k}_4}{6} + \mathrm{O}\left(h^5\right) \\ \mathbf{k}_1 &= h\dot{\mathbf{f}}\left(t_n, \mathbf{y}_n\right), \\ \mathbf{k}_2 &= h\dot{\mathbf{f}}\left(t_n + \frac{h}{2}, \mathbf{y}_n + \frac{\mathbf{k}_1}{2}\right), \\ \mathbf{k}_3 &= h\dot{\mathbf{f}}\left(t_n + \frac{h}{2}, \mathbf{y}_n + \frac{\mathbf{k}_2}{2}\right), \\ \mathbf{k}_4 &= h\dot{\mathbf{f}}\left(t_n + h, \mathbf{y}_n + \mathbf{k}_3\right) \end{aligned} \tag{C-4}$$

Both (C-3) and (C-4) restrict to the same (constant) time step $h$.

## APPENDIX D

### Crank-Nicolson method as applied

For the problem described by (C-1) and (C-2), the trapezoidal rule suggests using:

$$\begin{aligned} \mathbf{y}_{n+\beta} &= \left(1-\beta\right)\mathbf{y}_n + \beta\mathbf{y}_{n+1}, \\ \dot{\mathbf{y}}_{n+\beta} &= \left(\mathbf{y}_{n+1} - \mathbf{y}_n\right)/\Delta t \end{aligned} \tag{D-1}$$

and

$$\dot{\mathbf{f}}_{n\beta}\left(t, y\right) = \left(1-\beta\right)\dot{\mathbf{f}}_n + \beta\dot{\mathbf{f}}_{n+1} \tag{D-2}$$

Therefore, the system (C-1) is solved using the recursion:

$$\mathbf{y}_{n+1} = \mathbf{y}_n + h\left[\left(1-\beta\right)\dot{\mathbf{f}}_n + \beta\dot{\mathbf{f}}_{n+1}\right] \tag{D-3}$$

According to the choice of the parameter $\beta$ we distinguish four alternative schemes as follows:

$$\beta = \begin{cases} 0, & \text{forward difference / Euler} \\ 1/2, & \text{Crank-Nicolson (mid-point)} \\ 2/3, & \text{Galerkin} \\ 1, & \text{backward difference} \end{cases} \tag{D-4}$$

In this paper we have tested only the case of $\beta = 1/2$, which is the so-called Crank-Nicolson scheme. Moreover, since the

right-hand-side $\dot{\mathbf{f}}\left(t,\mathbf{y}\right)$ is a function of the unknown value $\mathbf{y}$, we have to start (D-3) for the initial given value $\dot{\mathbf{f}}_0$ at $t$=0, and then perform some iterations to update $\dot{\mathbf{f}}_{n+1}$, which is a function of $\mathbf{y}_{n+1}$. We distinguish two alternative schemes:

1) **Scheme 1**: We use the formula:

$$\mathbf{y}_{n+1} = \mathbf{y}_n + h\left(\dot{\mathbf{f}}_n + \dot{\mathbf{f}}_{n+1}\right)/2 \qquad \text{(D-5)}$$

and perform a number of iteration to determine the right-hand-side term $\left(\dot{\mathbf{f}}_n + \dot{\mathbf{f}}_{n+1}\right)/2$.

2) **Scheme 2**: As an alternative, we use the modified formula:

$$\mathbf{y}_{n+1} = \mathbf{y}_n + h\dot{\mathbf{f}}\left(t, \frac{\mathbf{y}_n + \mathbf{y}_{n+1}}{2}\right) \qquad \text{(D-6)}$$

and perform a number of iteration to determine the right-hand-side term $\dot{\mathbf{f}}\left(t, \frac{\mathbf{y}_n + \mathbf{y}_{n+1}}{2}\right)$.

## Author Introduction

**Christopher G. Provatidis** was born in Athens, Greece, in November 3, 1956. He has a BS in Mechanical-Electrical Engineering from the National Technical University of Athens, Greece (NTUA), 1977, a MSc in Mechanical Engineering from the NTUA, 1979 and a PhD also in Mechanical Engineering from the NTUA, 1987. The author's major field of study is applied mechanics.

He has experience in the design of steel structures (as IAESTE student, in the chemical industry SUPRA AB, Sweden, June-August, 1978). He served the Greek Army (Technical Branch 1980-1981) and then worked in projects concerning mechanical equipment of buildings and hospitals (1981-1982). In 1982, he moved to the National Technical University of Athens (NTUA) to work at the 'Machine Elements & Dynamics Laboratory'. He was appointed as Lecturer (1989-1993), Assistant Professor (1994-2002), Associate Professor (2002-2009) and he is currently Full Professor in the School of Mechanical Engineering at NTUA, Greece. In the same school, he served as a Vice-Chairman (2005-2007). He has participated in 35 European and national research projects. He has supervised over 120 diploma-works or MSc theses and eight PhD theses. He has written two books and three monographs (all in Greek). Over the past 30 years, he has worked across a wide discipline to include components of several sectors in mechanical simulation (elastostatics, crack and fatigue analysis, elastodynamics, acoustics, structural optimization, light-weight structures, textile micromechanics, thermal analysis, biomechanics: orthodontics, dental implants, orthopedics, inverse problems, system identification, gearless differentials, dynamics, CAD/CAE integration, etc) in conjunction with the finite element method, the boundary element method and other computational methods. As a result, he has more than 300 publications in refereed journals and conference proceedings. Current research interests include collocation methods, biomechanics and inertial propulsion, as well as rapid prototyping and other design tools.

Prof. Provatidis is a member of ASME, AIAA, European Society of Biomechanics (ESB), Greek Society of Biomechanics (Vice-president, 2008-2010), and Greek Association of Computational Mechanics (General Secretary, 2007-2009). In March 2011 he was elected as an active member (Class VI: Technical and Environmental Sciences) of the European Academy of Sciences and Arts (Salzburg, Austria).